Journal of the Korean Physical Society (2023) 83:43–51
https://doi.org/10.1007/s40042-023-00792-z

Online ISSN 1976-8524
Print ISSN 0374-4884

ORIGINAL PAPER - CONDENSED MATTER

Effects of substrate temperature and antireflection coating on the structural and optical properties of DC-sputtered chromium thin films for selective solar absorber applications

Justine J. Tibaijuka[1] · Justine S. Nyarige[2] · Mmantsae Diale[2] · Margaret E. Samiji[1] · Nuru R. Mlyuka[1]

Received: 9 January 2023 / Revised: 3 March 2023 / Accepted: 13 March 2023 / Published online: 29 March 2023

Abstract

The Cr and Cr/Al_xO_y thin films were deposited by DC sputtering onto soda lime glass and polished Al substrates at various deposition temperatures. The structural analysis of the multilayered coatings revealed a weak XRD diffraction peak at $2\theta \approx 43.3°$ ascribed to (110) plane of BCC structure of Cr metal. No phase of Al_xO_y was detected most likely due to the amorphous nature of the films. SEM and AFM analysis demonstrated the skewed distribution of small particles with an average surface roughness ranging between 4.0 and 13 nm. The optical analysis of the films revealed an increase in the steepness of the reflectance curve along the transition/plasma wavelength and blue shifting of this wavelength with the increase in substrate temperature. Also, a decrease in reflectance was observed upon employment of Al_xO_y antireflection coating as a result of shifting the transition wavelength toward longer wavelengths. These results suggest that substrate temperature and Al_xO_y antireflection coating are potential for improving the optical properties of Cr films for selective solar absorbers applications.

Keywords Chromium · Substrate temperature · Selective absorbers · Antireflection coating · Sputtering

1 Introduction

Concentrating solar power (CSP) technology, which requires an efficient selective solar absorber, is currently intensively researched as an alternative way to minimize the overdependence on limited, non-renewable, and eco-unfriendly fossil fuels. Ideally, the selective solar absorber surface, which is an essential part of CSP, should absorb all spectral solar radiation falling in it and emit none in the far-infrared range [1–3]. Along with solar selectivity, the selective coating should possess high hardness, structural and chemical stability, high-temperature stability, and high corrosion and oxidation resistance.

Among the materials researched for selective absorber coatings include intrinsic selective absorbers, such as Cr, V_2O_5, LaB6, Fe_3O_4, Al_2O_3, ZrB_2, ZrC, TaC, HfC, SiC, and ZrB_2 [4, 5]. Most of these materials' components are found in the lanthanide group or family of transition metals characterized by multiple orbital energy levels compatible with various wavelengths of visible light [4]. DC-sputtered Chromium (Cr) has been drawing significant attention from many researchers due to its tunable properties, including good adhesion, high melting point, high thermal conductivity, and high wear and corrosion resistance all of which are crucial in fabricating selective coating for high-temperature applications [6, 7]. Furthermore, the properties of Cr thin films can be engineered to suit diverse advanced technology device applications other than selective spectral absorption, such as photo masks, reticules and pinhole, on glass substrate integrated circuits and optical beam splitters, to mention a few [8, 9].

Unfortunately, Cr, like other intrinsic selective absorbers, lacks the steep reflectance spectra gradient on the cross-over/transition wavelength. Also, the transition (cross-over or plasma) wavelength of reflectance spectra in Cr selective absorber occurs at a shorter wavelength [4]. As a result, most of the radiation falling on the surface of the absorber gets lost due to reflection. On the other hand, absorbing maximum solar energy using intrinsic absorbers requires a thick layer which causes loss of energy through emittance. Some

✉ Justine J. Tibaijuka
jtibaijuka14@gmail.com; justine.tibaijuka@udsm.ac.tz

[1] Physics Department, University of Dar es Salaam, Uvumbuzi Road, P.O. Box 35063, Dar es Salaam, Tanzania

[2] Physics Department, University of Pretoria, Private Bag X20, Hatfield 0028, South Africa

of these challenges can be alleviated by employing structural or compositional engineering in the lattice of these materials, such as making composites with other materials or doping with a suitable donor, which gives rise to electron plasma and serves as scattering centers [4]. Also, multilayer configuration has been suggested for tuning Cr thin films' structural and optical properties [7]. Moreover, the spectral selectivity of DC-sputtered Cr thin films can be tailored through appropriate control of the deposition conditions, such as power, gas flow rates, the substrate to target distance, deposition rates and post-deposition heat treatment, among others [7, 9].

On the other hand, substrate temperature during deposition and the employment of antireflection (AR) coatings are among other factors reported to improve the optical properties of selective coatings. Antireflection coatings are usually applied on the top to enhance light transmission to the absorbing layers and minimize the loss of absorbed energy from the coating surface [1, 4]. So far, conventional AR coatings based on oxides and fluoride materials, such as Al_2O_3, SiO_2, HfO_2, Ta_2O_5, LaF_3, Er_2O_3, MgF_2, and NdF_3, have been researched and applied on several devices, such as spyglasses, lenses, displays, solar panels, cameras, and lasers [4]. Alumina films (Al_xO_y) are among the most potential antireflection coatings being used in several optical devices. The interest in it is driven by its feasible properties, such as full spectral transparency from ultraviolet to mid-infrared, tunable refractive index, good mechanical properties, and excellent thermal and chemical stability [5], which are potential for selective coating applications. Most importantly, aluminum oxide is characterized by some intrinsic selectivity, and thus its combination with Cr is ideal for selective coatings. Again, the substrate temperature is another potential factor reported to modify the films' optical properties as it influences the morphological parameters, such as roughness and grain size [4]. Despite the substantial progress made in exploring the selectivity of Cr films, the influence of substrate temperature and Al_xO_y AR coating on the spectral selectivity of DC-sputtered Cr thin films remain rarely addressed in the diverse open literature. This paper, therefore, presents a systematic study on the influence of substrate temperature and AR coating on the spectral selectivity of magnetron DC-sputtered Cr coating.

2 Experimental

2.1 Sample preparation

Cr and Al_xO_y thin films were respectively prepared onto Soda Lime Glass (SLG) and Aluminum substrate at various deposition temperatures between 25 and 300 °C by DC magnetron sputtering of Cr target (99.99%) and Al target (99.99%) commercially acquired from Plasmaterials Inc. In this study, the SLG substrate was selected to assess the optical transmittance and reflectance of Cr films, while the Al substrate was chosen to evaluate the spectral selectivity of Cr thin films. Before deposition, both the SLG and Al substrates were subjected to

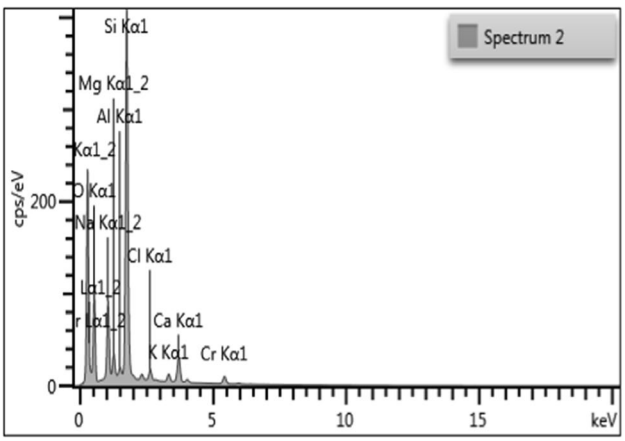

Fig. 2 EDX spectra of Cr films with Al_xO_y AR-coating (Cr/Al_xO_y) prepared on the SLG substrate

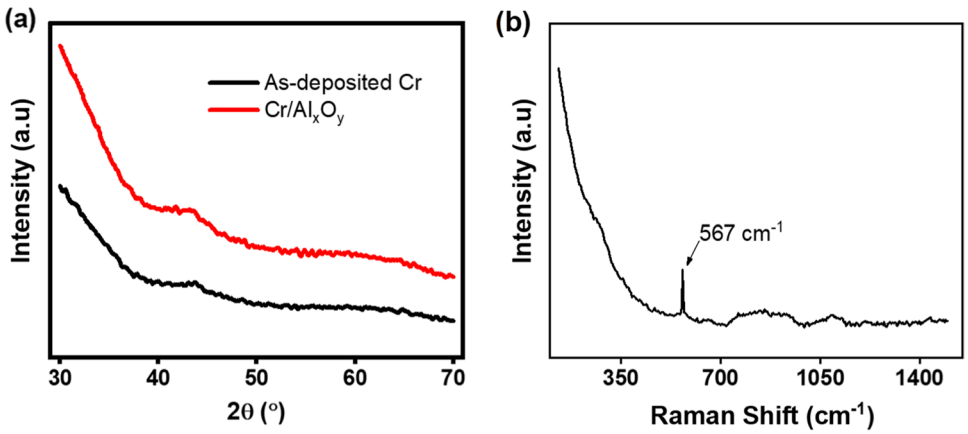

Fig. 1 The XRD spectra for as-deposited Cr layer and Cr/Al_xO_y thin films prepared on SLG substrates

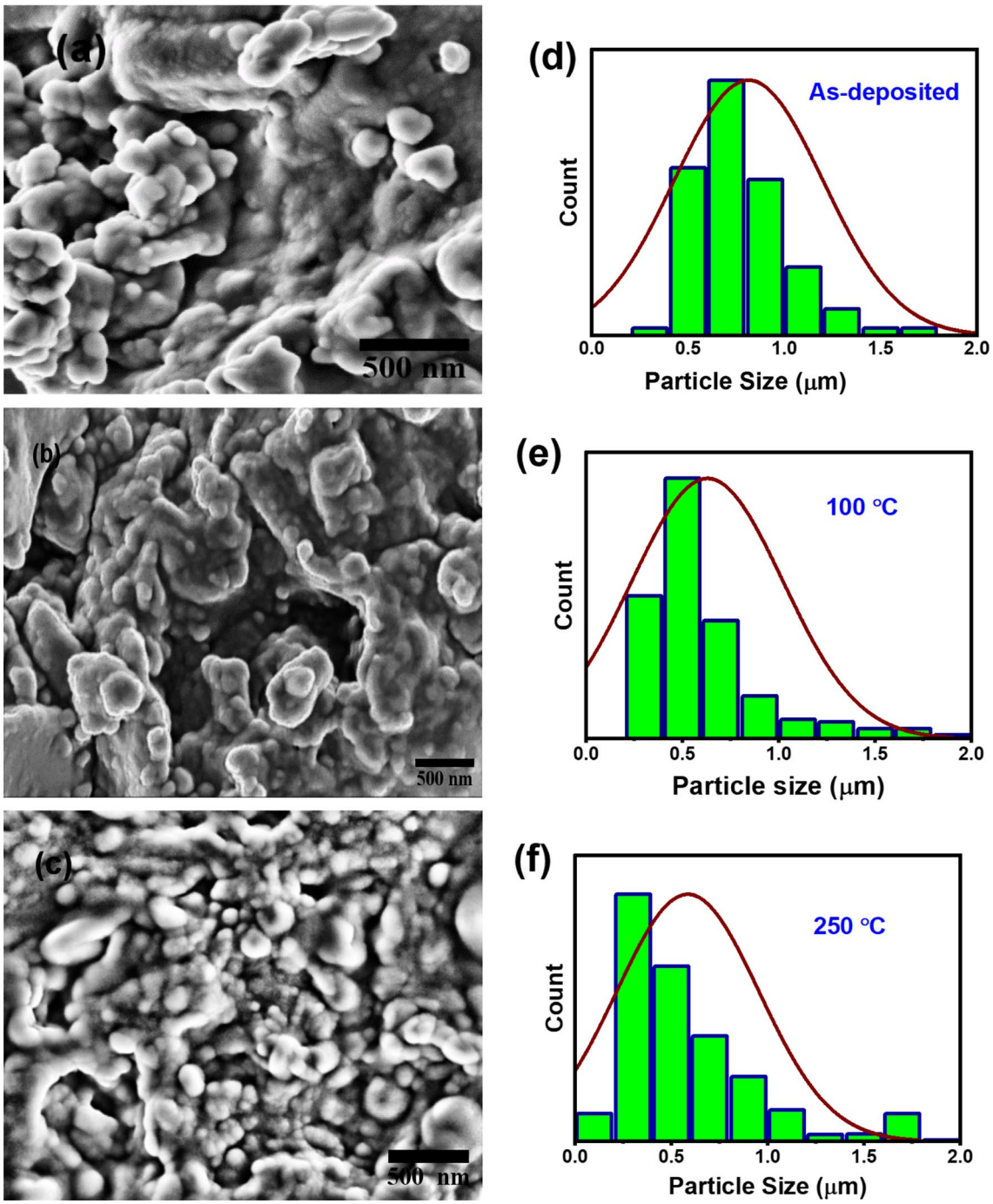

Fig. 3 SEM images and their corresponding grain size distribution for Cr films prepared on SLG substrate at different substrate temperatures; as-deposited (**a**, **b**), 100 °C (**c**, **d**) and 250 °C (**e**, **f**)

intensive cleaning to remove dust, grease, and other stacked contaminants on the substrates through ultrasonic cleaning, followed by rinsing in distilled water and ethanol before being suspended in ethanol vapor. Also, the BALZERS BAE 250 coating unit used for film preparation was evacuated to a base pressure of 7.0×10^{-6} mbar using the integrated turbo-molecular pump backed up with a rotary pump. The Cr films were sputtered at a power of 25 W and working pressure of 5.0×10^{-3} mbar using argon gas flowing at a rate of 15 SCCM as ascribed in Tibaijuka et al. [7]. Likewise, the Al_xO_y antireflection layers were reactively sputtered at a power of 200 W and working pressure of 5.0×10^{-3} mbar using argon and Oxygen gasses flowing at a rate of 75 SCCM and 4.15 SCCM, respectively. Additionally, the Al and Cr targets were

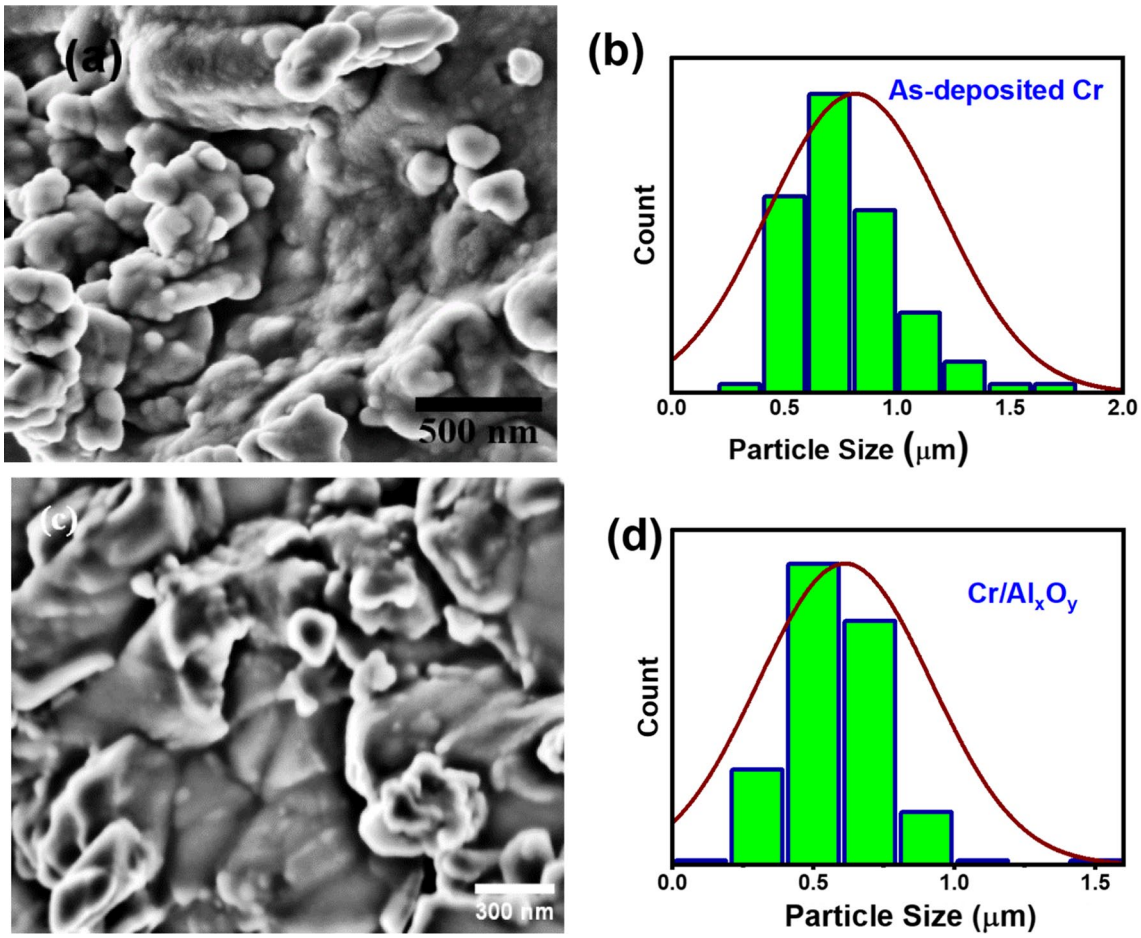

Fig. 4 SEM images and their corresponding grain size distribution of the as-deposited Cr and Cr/Al_xO_y prepared on SLG substrates

first pre-sputtered for 10 min to remove the target's surface contaminants and oxides before opening the shutter to begin the deposition on the substrates. During Al_xO_y deposition, the sputtering gas (Ar) was allowed to settle for 5 min; then, the reactive oxygen gas was gradually introduced into the chamber to minimize arcing.

2.2 Sample characterization

The films' thickness was determined by the Alpha step surface profiler through measuring the step created by the stacked Teflon tape on a substrate prior to deposition. The structural phase was characterized using a Bruker D2-Phaser X-ray Diffractometer (XRD) with Cu Kα radiation 1.5405 Å wavelengths at a scanning rate of 0.02° per second for the 2θ ranging from 20° to 70°. The resulting phases were identified with the help of reference PDF data available in the ICDD database. The surface morphology properties were analyzed using Zeiss Crossbeam 540 Field Emission-Scanning Electron Microscopy (FE-SEM) with electron acceleration voltage of 2 kV. Morphology was also analyzed by the Nanoscope IIIA multimode atomic force microscope in tapping mode. The resulting SEM and AFM images were analyzed for grain size distribution and surface roughness using ImageJ2 [10] and WSxM 4.0 software [11], respectively. The solar transmittance and reflectance spectra in the wavelength range $250 \leq \lambda \leq 2500$ nm were measured using Perkin Elmer Lambda 1050 + UV/VIS/NIR spectrophotometer.

3 Results and discussion

3.1 XRD analysis

Figure 1a portrays the XRD spectra of Cr thin films and that of Cr films with Al_xO_y antireflection coating (Cr/Al_xO_y) prepared on SLG substrates. It can be seen that there are low-intensity broad peaks due to the amorphous nature of the films. The distinct broad peak was observed at $2\theta \approx 43.3°$ which can be ascribed to the (110) plane of BCC Cr films (PDF#85-1336) [12]. In contrast, no significant XRD peaks attributed to Al_xO_y were present in samples with Al_xO_y AR

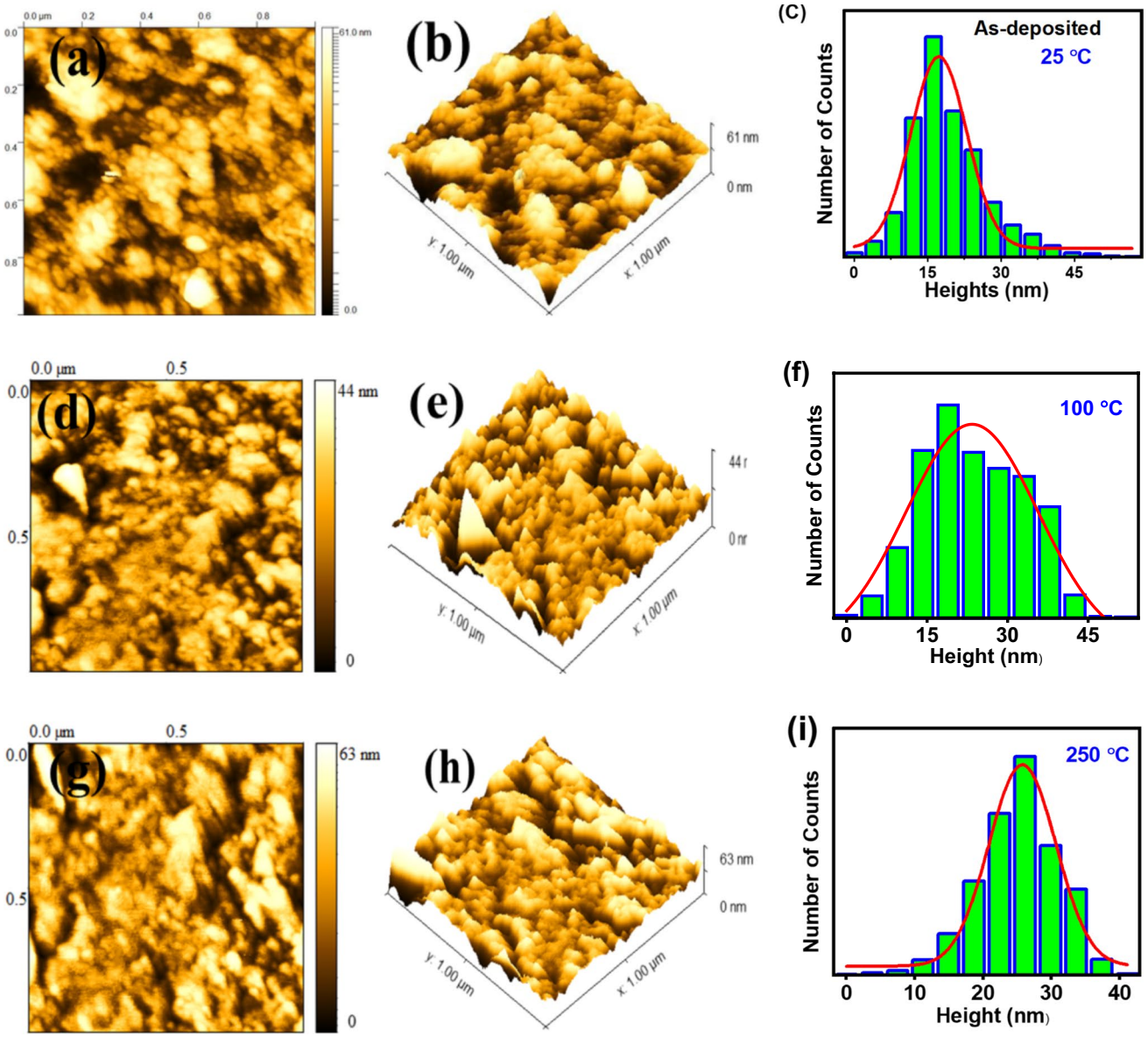

Fig. 5 2D and 3D AFM images with the corresponding height distributions for Cr films prepared on SLG substrate at different substrate temperatures; as-deposited (**a**–**c**), 100 °C (**e**–**g**) and 250 °C (**g**–**i**)

coatings. This is due to the fact that Al_xO_y usually crystallizes at higher temperatures, around 900 °C. Similar behavior corresponding to these results was previously reported in Cr and Al_xO_y films deposited at low power and substrate temperature [1, 12, 13]. Raman spectroscopy measurements on Cr/Al_xO_y presented in Fig. 1b revealed significant peak at 567 cm^{-1}, which is linked to Al–O vibration modes [14]. Figure 2 illustrates the EDX spectra of the Cr/Al_xO_y films deposited on the glass substrate. The EDX spectrum analysis showed the presence of Cr, Al, and O peaks at energies of 4.0 keV, 1.5 keV, and 0.52 keV, respectively, which is consistent with other literature [15]. Likewise, the other observed peaks likely arose from the glass substrate and a carbon coat on the samples that were deposited prior to taking SEM measurements.

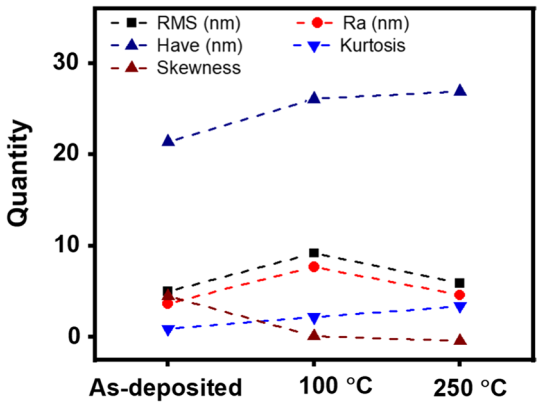

Fig. 6 AFM surface parameters for Cr prepared on SLG substrate at different substrate temperatures

3.2 SEM and AFM analysis

Figures 3 and 4 show SEM micrographs of the Cr films prepared on SLG substrates at different substrate temperature. The film grains distribution analysis shown in Figs. 3a and 4a revealed nearly normal grains distribution for the as-deposited Cr, and the distribution skewed to the left with increase in substrate temperature. Additionally, SEM images showed smaller grains, with an average size ranging from 6 to 8 nm and increased with the increase of substrate temperature. This trend could be associated with increased uniformity of the films with increased substrate temperature [15] as the increase in substrate temperature improves the mobility of the adatoms, thus facilitating surface diffusion and consequently, island growth [16]. Cr films with Al_xO_y AR coating showed uniformly distributed and relatively larger grains.

Figures 5 and 6 present 2D and 3D AFM topography and corresponding height distribution for Cr and Cr/Al_xO_y films prepared onto SLG substrate. As in SEM analysis, AFM images revealed a small cluster of grains which seems to decrease with substrate temperature. On the other hand, films with Al_xO_y antireflection (Fig. 7) showed uniformly and relatively larger grains, consistent with the SEM images. The results reveal further in Fig. 6 the average surface roughness (R_a) and root-mean-square roughness ranging between 4.0–8.0 nm and 5.0–6.0 nm, respectively, for Cr films deposited at different substrates temperatures; however, no clear trend was observed. Cr films with AR coating exhibited average roughness and RMS of 13.0 nm and 17.0 nm, respectively, which is relatively higher than their corresponding Cr films without AR coatings (Fig. 8). The average height distribution increased with substrate temperature from 22.0 to 27.0 nm for as-deposited samples and for samples deposited at 100–250 °C. The trend can be attributed to atoms migration due to substrate temperature increase, facilitating

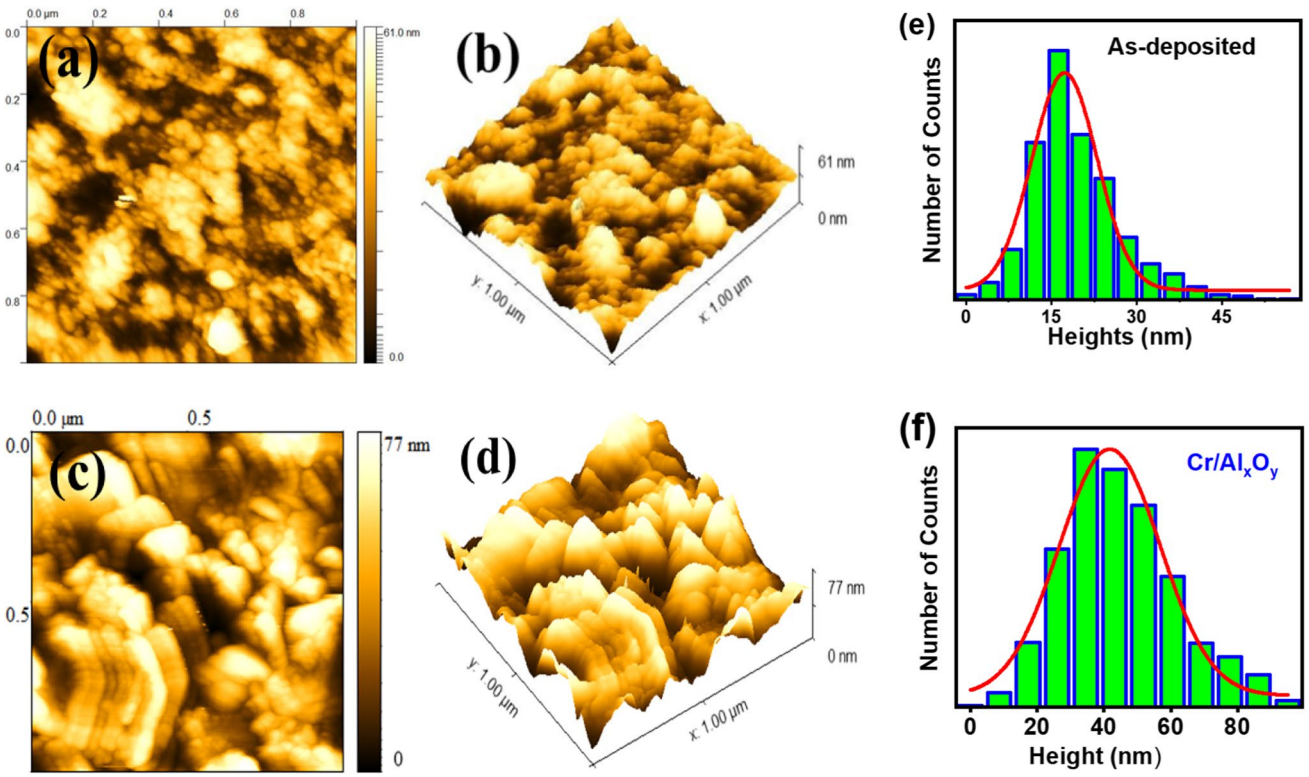

Fig. 7 2D and 3D AFM images with corresponding height distributions for (**a**, **b**, **e**) as-deposited Cr films and (**c**, **d**, **f**) Cr/AR-coating

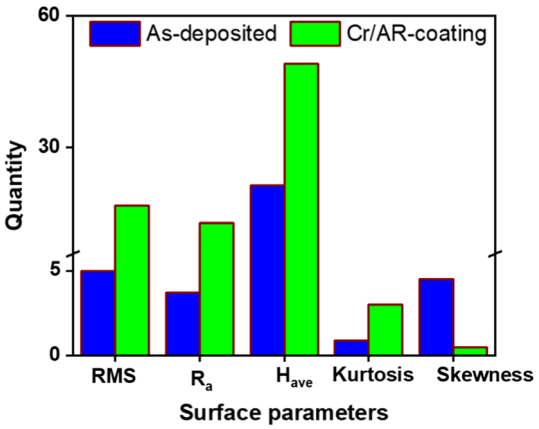

Fig. 8 AFM surface parameters for as-deposited Cr films and Cr with Al_xO_y AR-coating prepared on SLG substrates

the agglomeration of small particles into denser grains [15]. Average height distribution was found to be 49 nm for Cr films with Al_xO_y AR coatings.

In characterizing the symmetry and sharpness/peakedness of surface parameters, the height distribution analysis revealed the decrease of skewness from 3.4 to − 0.9 and the spontaneous increase in kurtosis values from 0.9 to 3.4 with the increase of substrate temperature. This trend signifies the increase of peaks' sharpness and valleys on the film surface with increased substrate temperature [7, 17–19]. Based on these results, it is evident that the substrate temperature influences the surface parameters of the films, and thus they are potential for enhancing the grains and roughness parameters of the films, which is beneficial for selective solar absorber surface engineering. Besides, the kurtosis and the skewness values of 3 and 0.49, respectively, were recorded for Cr films with Al_xO_y AR coatings (Fig. 8), indicating that broader peaks dominated the surface of the film.

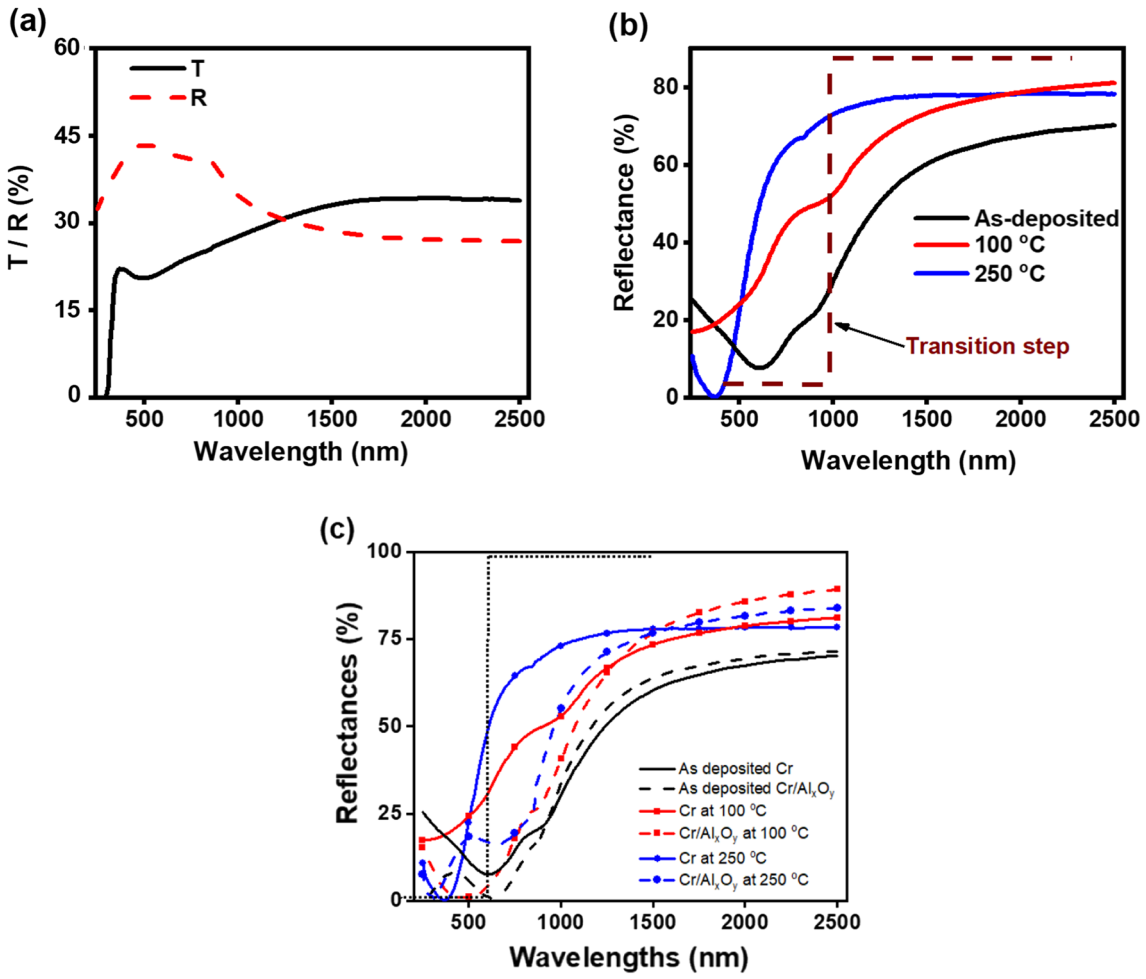

Fig. 9 Optical transmittances and reflectance of Cr films prepared on **a** SLG substrate, **b** Al substrate at different substrate temperatures, **c** Al substrate with Al_xO_y AR coating

3.3 Optical properties

Figure 9 shows the optical transmittances and reflectance of Cr and Cr films with Al_xO_y prepared on glass and aluminum substrates. As reported in the previous study [7], Cr thin films on glass substrates exhibited a relatively high transmittance in the infrared region compared to the visible part of the solar spectrum. Meanwhile, the reflectance was higher in the visible spectrum and decreased gradually with the increase in wavelengths. The average transmittance (T_{ave}) was computed using Eq. (1) adopted from Ollotu et al. [18] at the Air Mass 1.5 solar irradiance $G(\lambda)$. As shown in Fig. 9a, the average transmittance was found to be ~25%, while the reflectance was above 39%, which is appropriate for selective solar absorber applications.

$$T_{ave} = \frac{\sum_{250}^{2500} T(\lambda)G(\lambda)}{\sum_{250}^{2500} G(\lambda)} \quad (1)$$

For the films deposited on a polished aluminum substrate, low reflectance was observed in the wavelength range of ~250–750 nm before increasing abruptly in the wavelength range above 750 nm, which signifies more light is being absorbed in shorter wavelength and more light reflection in the longer wavelengths, hence spectral selectivity. Similarly, the steepness of the curve along the transition wavelength increased with the increase in substrate temperature, which indicates the drifting of the transition wavelength (cross-over wavelength) toward the shorter wavelength with the increase in substrate temperature. This trend could be associated with improved homogeneity on the film surfaces, as revealed by the decrease in surface roughness in AFM analysis. Furthermore, the Al_xO_y antireflection coating drifted the transition wavelength (cross-over wavelength) toward the longer wavelength, signifying the improvement in spectral selectivity. With these results, it is worth mentioning that the substrate temperature and the antireflection coating can be used to engineer the selectivity of selective solar absorbers.

4 Conclusions

The Cr films and Cr with Al_xO_y AR coating were successfully fabricated through DC sputtering onto soda lime glass and polished Al substrate at various substrate temperatures. The structural analysis of the coatings revealed a low crystalline peak at $2\theta \approx 43.3°$ corresponding to (110) plane of BCC Cr films; however, no Al_xO_y diffraction peak was observed due to the amorphous nature of the films. SEM and AFM analysis revealed skewed distributed small particles with an average size of 6.0–8.0 nm and surface roughness of 4.0–13 nm. The optical analysis of the coating shows an increase in the steepness of the curve along the transition wavelength with the increase of substrate temperature, which signifies the drifting of transition wavelength toward the shorter wavelengths. Further decrease of the reflectance was observed upon employing the Al_xO_y antireflection coating, indicating the drifting of transition wavelength toward the longer wavelengths which is desired for selective solar absorbers. These results suggest that substrate temperature and Al_xO_y antireflection coating can potentially enhance the optical properties of Cr thin films for selective solar absorbers applications.

Acknowledgements The Tanzanian Ministry of Education, Science, and Technology (MoEST) is sincerely appreciated for providing JT with a scholarship. The authors also acknowledge the University of Dar es Salaam, the University of Pretoria, the Materials Science and Solar Energy Network for Eastern and Southern Africa (MSSEESA), SARCHI UID No.115463, and the International Science Program (ISP) at Uppsala University for providing research facilities and materials as well as logistical and financial support during JT lab's stay at Pretoria University.

Author contributions All authors, except JSN contributed to the study conceptualization. Sample preparation, data collection, and analysis were conducted by JJT. JSN participated in SEM, Raman and XRD characterization. NRM, MD, and MES handled financial acquisition and supervision of work. JJT wrote the initial draft of the manuscript, and all of the other authors reviewed and edited the earlier draft. The final manuscript was read and approved by all authors.

Funding This study was jointly supported by the Ministry of Education, Science and Technology of Tanzania (MoEST), the University of Dar es Salaam, University of Pretoria, Materials Science and Solar Energy network for Eastern and Southern Africa (MSSEESA), SARCHI UID No.115463 and the International Science Program (ISP)—Uppsala University.

Data availability Datasets related to this article data will be made available upon reasonable request.

Declarations

Conflict of interest The authors declare no conflict of interest.

References

1. N. Khoza et al., J. Alloys Compd. (2019). https://doi.org/10.1016/j.jallcom.2018.09.329
2. A.B. Khelifa et al., J. Alloys Compd. (2019). https://doi.org/10.1016/j.jallcom.2018.12.286
3. A. Al-Rjoub et al., Sol. Energy (2018). https://doi.org/10.1016/j.solener.2018.04.052
4. A. Dan, H.C. Barshilia, K. Chattopadhyay, B. Basu, Renew. Sustain. Energy Rev (2017). https://doi.org/10.1016/j.rser.2017.05.062
5. N. Reddy et al., Ceram. Int. (2014). https://doi.org/10.1016/j.ceramint.2014.03.133
6. X.Z. Wang, H.Q. Fan, T. Muneshwar, K. Cadien, J.L. Luo, J. Mater. Sci. Technol. (2021). https://doi.org/10.1016/j.jmst.2020.06.012

7. J.J. Tibaijuka, M.E. Samiji, M. Diale, N.R. Mlyuka, Tanzan. J. Sci. (2022). https://doi.org/10.4314/tjs.v48i3.13
8. K. Rauf, F. Ahmed, A. Nasim, N. Khan, A. Gul, IOP Conf. Ser. Mater. Sci. Eng. (2016). https://doi.org/10.1088/1757-899X/146/1/012013
9. J. Peralta, J. Esteve, A. Lousa, Thin Solid Films (2020). https://doi.org/10.1016/j.tsf.2019.137676
10. C.T. Rueden et al., BMC Bioinform. (2017). https://doi.org/10.1186/s12859-017-1934-z
11. I. Horcas et al., Rev. Sci. Instrum. (2007). https://doi.org/10.1063/1.2432410h
12. S.F. Wang, H.C. Lin, H.Y. Bor, Y.L. Tsai, C.N. Wei, J. Alloys Compd. (2011). https://doi.org/10.1016/j.jallcom.2011.08.052
13. Z.Y. Nuru, C.J. Arendse, T.F.G. Muller, M. Maaza, Mater. Sci. Eng.: B. (2012). https://doi.org/10.1016/j.mseb.2012.05.028
14. T. Sudare, Cryst. Eng. Comm. (2019). https://doi.org/10.1039/C9CE01064E
15. Z.Y. Nuru et al., Renew. Energy (2015). https://doi.org/10.1016/j.renene.2014.10.050
16. R. Balu, A.R. Raju, V. Lakshminarayanan, S. Mohan, Mater. Sci. Eng.: B. (2005). https://doi.org/10.1016/j.mseb.2005.06.021
17. O. Malik, F.J. De la Hidalga-Wade, J. Mater. Res. (2015). https://doi.org/10.1557/jmr.2015.159
18. E.R. Ollotu, J.S. Nyarige, N.R. Mlyuka, M.E. Samiji, M. Diale, J. Mater. Sci. Mater. Electron. (2020). https://doi.org/10.1007/s10854-020-04192-y
19. J.J. Tibaijuka, J.S. Nyarige, M. Diale, N.R. Mlyuka, M.E. Samiji, J. Mater. Sci. Mater. Electron. (2023). https://doi.org/10.1007/s10854-022-09571-1